Supplementary Materials for

Improved Teflon Lift-Off for Droplet Microarrays Generation and Single-Cell Separation on Digital Microfluidic Chips

Chuanjie Shen,[1,2] Zhaoduo Tong,[1,2] Xin Xu, [1] and Hongju Mao[1,2*]

1. *State Key Laboratory of Transducer Technology, Shanghai Institute of Microsystem and Information Technology, Chinese Academy of Sciences, Shanghai 200050, China.*
2. *Center of Materials Science and Optoelectronics Engineering, University of Chinese Academy of Sciences, Beijing, 100049, China.*

* Hongju Mao
E-mail: hjmao@mail.sim.ac.cn; Fax: +86 21 62511070 8714; Tel: +86 21 62511070 8701

This PDF file includes:

Figs. S1 to S11
Table S1 to S3
Videos S1 to S3

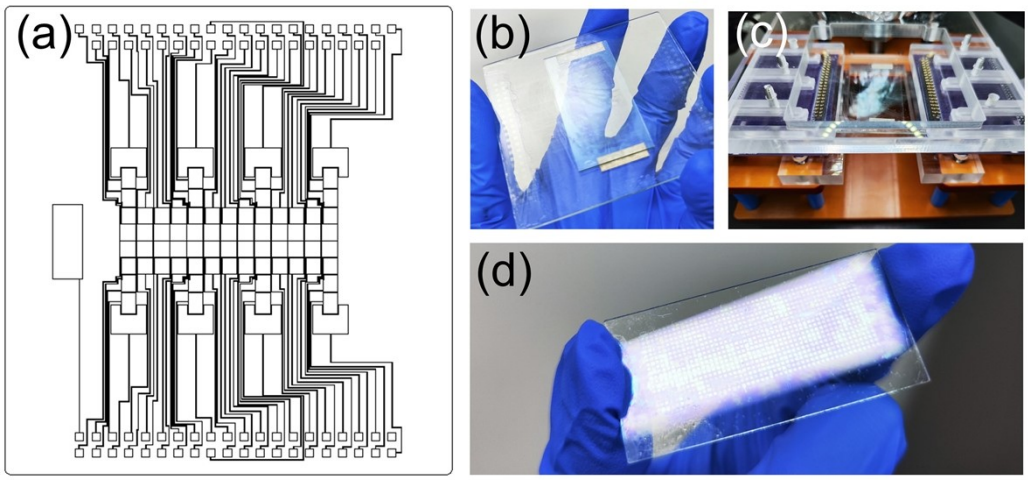

Figure S1. (a) The electrode pattern design of the DMF bottom plate. (b) Physical image of the DMF chip. (c) Custom-designed holder for the chip connected with the DMF control system. (d) Hydrophilic-hydrophobic arrays located on the upper plate.

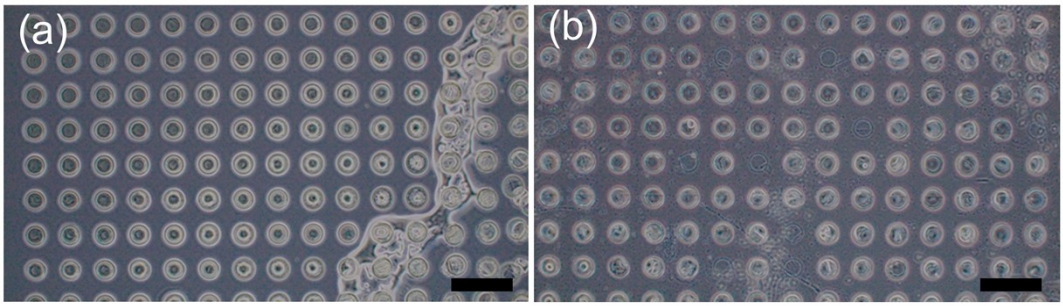

Figure S2. (a) The Teflon layer on the untreated ITO glass surface was eroded and damaged by acetone. (b) After coating a hydrophilic layer on the ITO surface, the Teflon layer adheres stably. Scale bars are 500 μm.

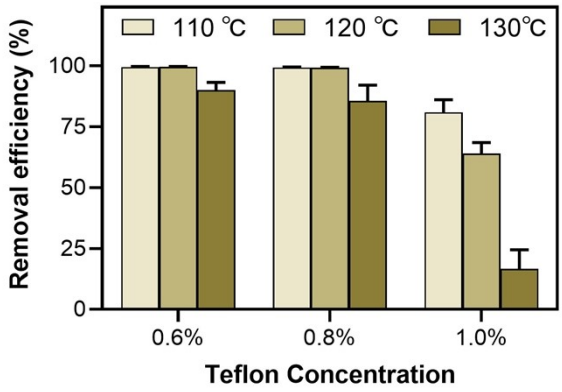

Figure S3. Characterization of the Teflon lift-off process with the removal efficiency of 99.5% (0.6%, 110 °C), 99.3% (0.6%, 120 °C), 90.0% (0.6%, 130 °C), 99.2% (0.8%, 110 °C), 99.1% (0.8%, 120 °C), 85.6% (0.8%, 130 °C), 80.9% (1.0%, 110 °C), 63.9% (1.0%, 120 °C), and 16.7% (1.0%, 130 °C), respectively.

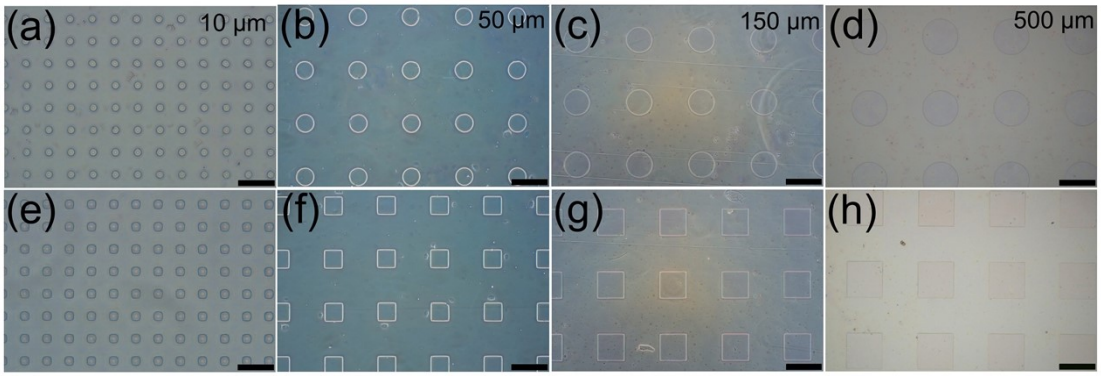

Figure S4. (a)-(d) Circular spots with the diameter of 10, 50, 150, and 500 μm, respectively. (e)-(h) Square spots with the side length of 10, 50, 150, and 500 μm, respectively. Scale bars: 50 μm for (a) and (e); 100 μm for (b) and (f); 200 μm for (c) and (g); 500 μm for (d) and (g).

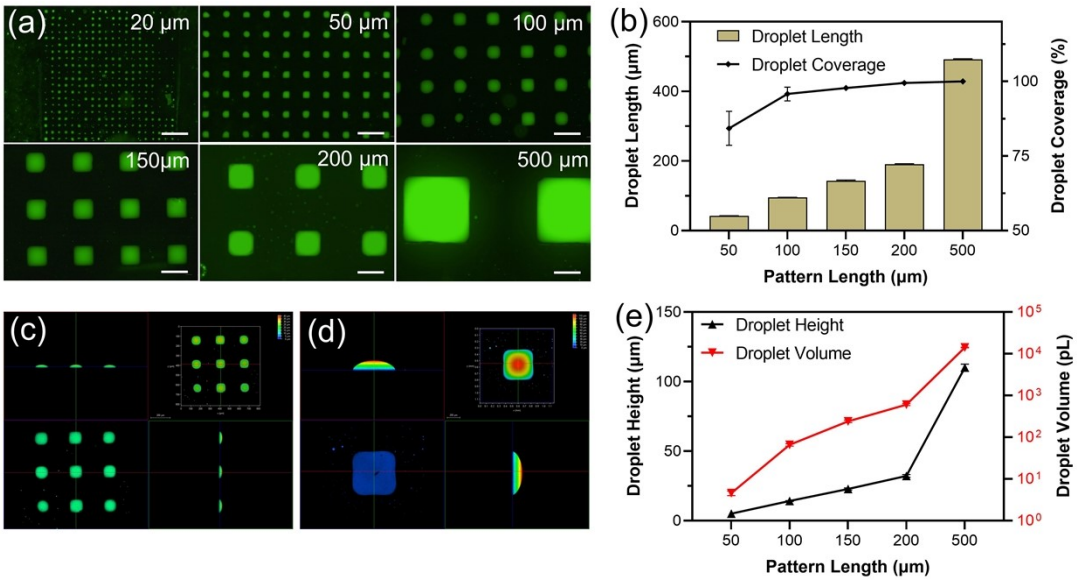

Figure S5. Characterization of square droplets generated by MDA-DMF. (a) Fluorescent images of micro droplets which are 20, 50, 100, 150, 200, 500 μm in size length, respectively. Scale bars are 200 μm. (b) The side length and coverage of droplets varies with patterns size length. (c), (d) Sectional views of the droplets formed on square patterns by 100 μm and 500 μm, respectively. (e) Effect of the size of the square patterns on the height and volume of droplets.

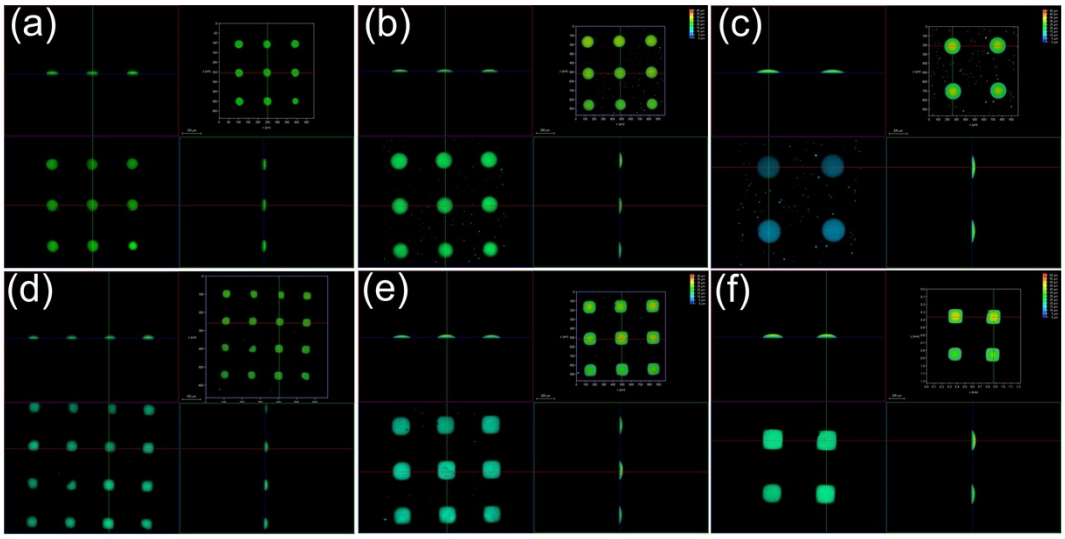

Figure S6. Sectional views of the droplets formed on circular patterns of (a) 50 μm, (b) 150 μm, and (c) 500 μm, respectively, and on square patterns of (d) 50 μm, (e) 150 μm, and (f) 500 μm, respectively.

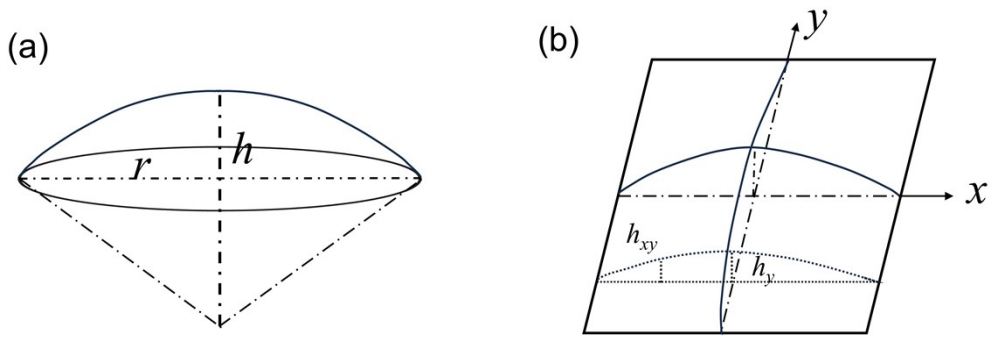

Figure S7. Sketches of the microdroplet volume calculation for (a) circular droplets and (b) square droplets, respectively.

Calculation of circular microdroplets' volume[1]. For the circular microdroplet considered as a spherical cap structure, the volume could be calculated by equation:

$$V = \frac{\pi h}{6}(3r^2 + h^2) \tag{1}$$

where *r* was the radius of the hydrophilic site, *h* was the height of the microdroplet, respectively.

Calculation of square microdroplets' volume[2]. For the square bottom microdroplet, the surface projection was considered to be a circular arc shape, so the volume could be calculated by equations:

$$h_{xy} = \sqrt{\left(\frac{r^2 + h_y^2}{2h_y}\right)^2 - x^2} - \frac{r^2 - h_y^2}{2h_y} \tag{2}$$

$$S_y = \int_{-r}^{r} h_{xy}\mathrm{d}x = 2\int_{-r}^{0} h_{xy}\mathrm{d}x \tag{3}$$

$$V = \int_{-r}^{r} S_y\mathrm{d}y = 4\int_{-r}^{0}\int_{-r}^{0}\left(\sqrt{\left(\frac{r^2 + h_y^2}{2h_y}\right)^2 - x^2} - \frac{r^2 - h_y^2}{2h_y}\right)\mathrm{d}x\mathrm{d}y \tag{4}$$

$$h_y = \sqrt{\left(\frac{r^2 + h^2}{2h}\right)^2 - y^2} - \frac{r^2 - h^2}{2h} \tag{5}$$

where *r* was half the side length of the bottom, *h* was the height of the microdroplet, respectively.

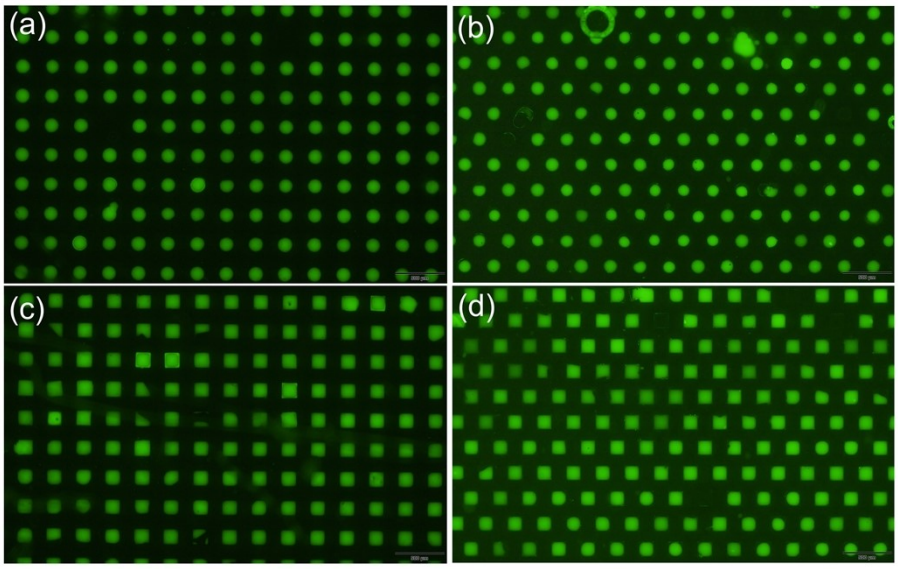

Figure S8. Arrays of (a) circular and (c) square droplets arranged in a 300 μm square grid. Arrays of (b) circular and (d) square droplets arranged in a 300 μm triangular grid. Scale bars are 500 μm.

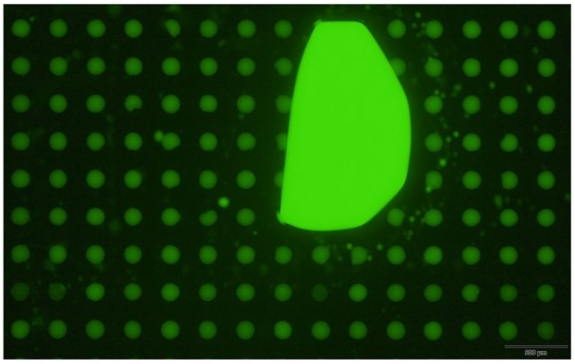

Figure S9. The residual of the mother droplet during the generation of MADs on DMF chip. Scale bars is 500 μm.

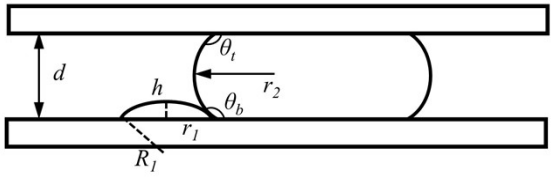

Figure S10. Sketch of the effect of the thickness for droplet generation.

Stress analysis of the droplet splitting process. During the process of droplet splitting, the pressure inside the microdroplet (P_1) was approximately equal to that of the mother droplet (P_2):

$$P_1 = P_2 \tag{6}$$

For the microdroplet considered as a spherical cap structure, P_1 could be calculated by the Laplace's equation[2]:

$$P_1 = \frac{2\gamma}{R_1} = \frac{2\gamma}{\frac{r_1^2 + h^2}{2h}} = \frac{4\gamma h}{r_1^2 + h^2} \tag{7}$$

where γ was the surface tension, R_1 was the curvature radius of the microdroplet, r_1 was the radius of the hydrophilic site, h was the height of the microdroplet, respectively.

For the Laplace Pressure of the mother droplet, P_2 could be calculated by the Laplace's equation[3]:

$$P_2 = \gamma\left(\frac{1}{r_2} + \frac{1}{R_2}\right) \tag{8}$$

where R_2 was the principal curvature radius in the horizontal direction, r_2 was the principal curvature radius in the vertical direction. According to the geometric relationship:

$$r_2 = \frac{-d}{\cos\theta_t + \cos\theta_b} \tag{9}$$

where d was the spacer thickness, θ_t and θ_b were the contact angles of the mother droplet on the upper and lower plates, respectively.

It can be seen that bigger d resulted in larger r_2 and R_1, which resulted in smaller h, corresponding to a smaller microdroplet.

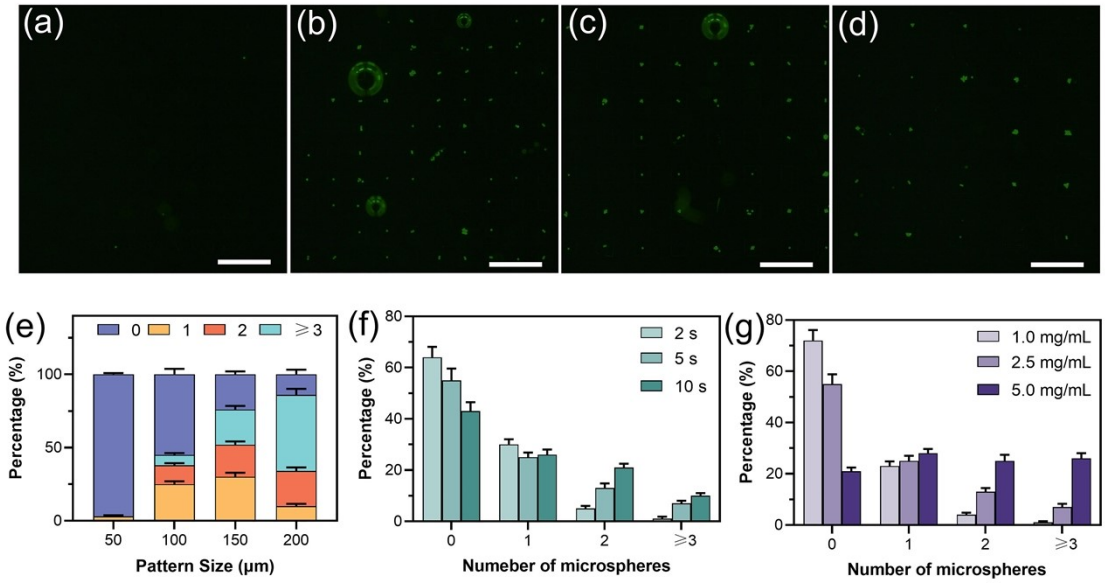

Figure S11. Fluorescent images illustrating the microsphere distributions on MDA-DMF with hydrophilic patterns of (a) 50 μm; (b) 100 μm; (c) 150 μm; and (d) 200 μm. Scale bars are 500 μm. (e) Distribution of the microsphere numbers on the microarrays with 50, 100, 150, and 200 μm hydrophilic patterns. The single-microsphere dispersion rates are 2%, 25%, 30%, and 10%, respectively. (f) Distribution of isolated microspheres on 150-μm microarrays with different settling time of 2, 5, and 10 seconds. (g) Distribution of isolated microspheres on 150-μm microarrays with different concentration of 1.0, 2.5, and 5.0 mg/mL.

Table S1. Statistics of the data of the droplets with different sizes.

Pattern size (μm)		Droplet size (μm)	Droplet height (μm)	Droplet volume (pL)	Droplet CV	Droplet coverage	Minimum voltage (V)
Circular spots	50	41.18±0.54	3.38±0.46	2.28±0.36	15.72%	75.7±10.6%	122±2
	100	89.78±1.54	12.49±0.86	40.61±3.92	9.66%	92.8±3.2%	125±1
	150	140.73±2.12	19.50±0.98	155.46±10.57	6.80%	96.5±1.0%	130±5
	200	189.94±2.53	29.40±1.25	429.87±20.35	4.73%	98.1±0.4%	140±4
	500	490.00±3.80	101.65± 2.14	10130.53± 269.05	2.66%	100.0±0.0%	168±8
Square spots	50	42.25±0.44	5.03±0.58	4.57±0.69	12.25%	84.3±5.7%	123±1
	100	92.02±0.79	14.14±0.66	65.72±5.02	7.64%	95.8±2.2%	128±3
	150	143.23±1.91	22.75±0.80	241.19±15.89	6.58%	97.0±1.0%	138±4
	200	190.75±1.47	32.15±1.02	607.00±25.56	4.21%	98.5±0.2%	152±4
	500	491.50±2.29	110.00± 2.51	14176.81± 304.36	2.15%	100.0±0.0%	185±7

Table S2. Statistics of the data of the microsphere isolation.

Parameters		Number of microspheres per droplet			
		0	1	2	≥3
Pattern size (μm)	50	97%	3%	0	0
	100	55%	25%	13%	7%
	150	24%	30%	22%	24%
	200	14%	10%	24%	52%
Settling time (s)	2	64%	30%	5%	1%
	5	55%	25%	13%	7%
	10	43%	26%	21%	10%
Concentration (mg/mL)	1.0	72%	23%	4%	1%
	2.5	55%	25%	13%	7%
	5.0	21%	28%	25%	26%

Table S3. Statistics of the data of the cell isolation.

Parameters		Number of cells per droplet			
		0	1	2	≥3
Pattern size (μm)	50	97%	3%	0	0
	100	45%	28%	15%	12%
	150	29%	27%	17%	27%
	200	0	0	2%	98%
Settling time (s)	2	64%	23%	9%	4%
	5	45%	28%	15%	12%
	10	33%	25%	20%	22%
Concentration (/mL)	2.5×10^6	56%	29%	10%	5%
	5.0×10^6	45%	28%	15%	12%
	1.0×10^7	20%	35%	26%	19%

Movie S1. The generation of micro droplets in air medium.

Movie S2. The generation of micro droplets in oil medium.

Movie S3. The distribution of cells on DMA-DMF.

References

1. A. A. Popova, K. Demir, T. G. Hartanto, E. Schmitt and P. A. Levkin, *Rsc Advances*, 2016, **6**, 38263-38276.
2. H. Li, Q. Yang, G. Li, M. Li, S. Wang and Y. Song, *ACS Appl Mater Interfaces*, 2015, **7**, 9060-9065.
3. C. Sung Kwon, M. Hyejin and K. Chang-Jin, *Journal of Microelectromechanical Systems*, 2003, **12**, 70-80.